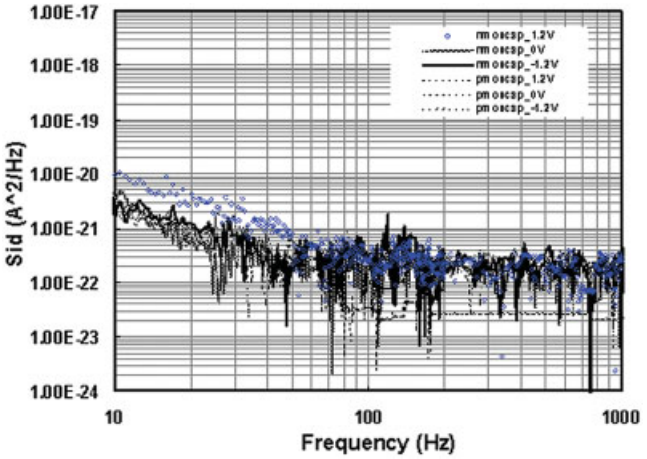

Figure 4 The measured flicker noise has a relationship with the frequency for 65 nm NMOS and PMOS varactors. [Color figure can be viewed in the online issue, which is available at www.interscience.wiley.com]

passed from the C_{gate} to the bulk ground. In Figure 4, the measured MOS varactor flicker noise, where the dimensions of $W \times L \times G \times B = 1.6 \times 0.4 \times 8 \times 64$, has presented a different flicker noise level at 1.2 V as a result of the leakage current being one order of magnitude higher compared with other DC bias conditions. This can be explained by the fact that an increased modeling parameter for I_{gate} results in an increased leakage current of NMOS varactor at 1.2 V. It was noticed that there was an increase in noise when the current was higher than 10^{-4} mA. This phenomenon did not occur when the leakage current is 10^{-5} and 10^{-6} mA at -1.2 and 0 V, respectively, Also, I_{gate} changes the flicker noise level, as I_{gate} rises above than 10^{-4} mA. Moreover, it was found that measured results for PMOS varactor are always lower than 10^{-5} mA between the -1.2 and 1.2 V, so would have no impact on the noise level variation. Although the measured noise of MOS varactor has a lower level than the one created by MOSFET, adding the fitting parameters to the simulator is an unavoidable trend as noise level rapidly increases with increased leakage current.

5. CONCLUSIONS

In this study, we investigated the optimum 65 nm LP MOS varactors geometrical relation in terms of microwave characteristics and low frequency noise performances. The equivalent circuit model also achieves precisely extracting parasitic parameters and agrees with measured results. The I_{gate} parameter of the MOS varactor model also can be validated as a relationship with flicker noise on MOS varactor.

ACKNOWLEDGMENTS

This work is financially supported by the Taiwan Semiconductor Manufacturing Company.

REFERENCES

1. J. Maget, M. Tiebout, and R. Kraus, MOS varactors with n- and p-type gates and their influence on an LC-VCO in digital CMOS, IEEE J Solid State Circ 38 (2003), 1139–1147.
2. C.S. Chun, Y.G. Zhou, K.J. Chen, and K.M. Lau, Q-factor characterization of RF GaN-based metal-semiconductor-metal planar interdigitated varactor, IEEE Trans Electron Dev 26 (2005), 432–434.
3. C.F. Huang, C.C. Wu, C.H. Chen, C.C. Ho, Y.J. Chan, C.S. Chang, et al., A comprehensive varactor study for advanced CMOS RFIC design, IEEE VLSITSA (2005), 66–67.
4. A. Dec and K. Suyama, A 1.9-GHz CMOS VCO with micromachined electromechanically tunable capacitors, IEEE J Solid State Circ 35 (2000), 1231–1237.
5. W.M.Y. Wong, P.S. Hui, Z.H. Chen, K.Q. Shen, J. Lau, P.C.H. Chan, et al., A wide tuning range gated varactor, IEEE J Solid State Circ 35 (2000), 773–779.
6. F. Hur, Z.H. Chen, K.Q. Shen, J. Lau, M. Huang, M.S. Chan, et al., High-Q SOI gated varactor for use in RF ICs, IEEE Int SOI Conf (1998), 31–32.
7. S. Levantino, C. Samori, A. Bonfanti, S.L.J. Gierkink, A.L. Lacaita, and V. Boccuzzi, Frequency dependence on bias current in 5-GHz CMOS VCOs: Impact on tuning range and Flicker noise upconversion, IEEE J Solid State Circ 37 (2002), 1003–1011.
8. A. Hajimiri and T.H. Lee, A general theory of phase noise in electrical oscillators, IEEE J Solid State Circ 33 (1998), 179–194.
9. N. Itoh, S. Ishizuka, and K. Katoh, Integrated LC-tuned VCO in BiCMOS process, Solid State Circ Conf, San Francisco, CA (2001), 329–332.

DESIGN OF A STOPBAND-IMPROVED UWB FILTER USING A PAIR OF SHUNT AND EMBEDDED OPEN STUBS

Min-Hang Weng,[1] Hon Kuan,[2] Wen-Lang Chen,[2] Chang-Sin Ye,[3] and Yan-Kuin Su[3]
[1] Medical Devices and Opto-Electronics Equipment Department, Metal Industries Research and Development Center, Taiwan
[2] Department of Technology Electro-Optical Engineering, Southern Taiwan University, Taiwan
[3] Department of Electrical Engineering, Advanced Optoelectronic Technology Center, Institute of Microelectronics, National Cheng Kung University, Taiwan; Corresponding author: peacemaker1983@gmail.com

Received 3 December 2008

ABSTRACT: *In this letter, an ultrawideband (UWB) bandpass filter (BPF) with an improved stopband has been proposed. The proposed UWB BPF, having a lower passband of 3.5–5.2 GHz and a higher passband of 6.5–9.7 GHz, mainly comprises the parallel-coupled lines and slot-line resonator. A wide stopband of the proposed BPF from 10 to 20 GHz can be achieved by using a pair of shunt and embedded open stubs. The proposed UWB BPF is designed, fabricated, and measured. Good agreement with the electro-magnetic simulation and measurement is demonstrated.* © 2009 Wiley Periodicals, Inc. Microwave Opt Technol Lett 51: 2121–2124, 2009; Published online in Wiley InterScience (www.interscience.wiley.com). DOI 10.1002/mop.24556

Key words: *ultrawideband (UWB); bandpass filter (BPF); parallel-coupled lines; slot-line resonator (SLR); bandstop filter (BSF)*

1. INTRODUCTION

Since the U.S. Federal Communications Commission proposed the unlicensed use of ultrawideband (UWB) (range of 3.1–10.6 GHz) for commercial purposes in early 2002 [1], the UWB bandpass filter (BPF) has been investigated extensively. Recently, several methods for designing UWB BPFs have been proposed, such as multiple-mode resonator [2], stepped-impedance resonator (SIR) [3], parallel coupled line [4], or slot-line structure [5–8]. For example, a UWB BPF is proposed by using two microstrip open-circuited stubs coupled to a single CPW resonator on the other side of a commercial substrate [5]. Additionally, a notch band is needed

to avoid the existing band of 5–6 GHz used for wireless local area network. Therefore, some UWB BPFs with a notch band by using an embedded open stub or spurline to create an attenuation pole of 5–6 GHz have been reported [9, 10]. Although various kinds of bandstop structure, such as SIR [11], spurline [12], and defect ground-structure [13] have been developed to remove or suppress the higher-order harmonics and other unwanted spurious signals of the BPFs. However, there are few papers concerning about the bandstop improvement of the UWB BPF.

Therefore, in this study, we reported a UWB BPF with a deep and wide stopband rejection greater than 23 dB from 10 to 20 GHz. The proposed UWB BPF mainly contains the parallel-coupled lines and slot-line resonator (SLR). By using a pair of shunt and embedded open stubs as the bandstop filter (BSF), the stopband of the proposed UWB BPF is much improved without affecting the passband performance. The shunt open stubs and the embedded open stubs have electrical lengths of quarter-wavelength and low characteristic impedance to enlarge the stopband range. The proposed UWB BPF is designed, fabricated, and measured. The used substrate for simulation and fabrication is RT/Duroid 5880 with a dielectric constant of $\varepsilon_r = 2.2$, a loss tangent of 0.0009, and a thickness h of 0.508 mm. Good agreement between the electromagnetic (EM) simulation and measurement is verified.

2. FILTER STRUCTURE AND DESIGN PROCEDURE

Figure 1 shows the configurations of the proposed UWB filter with a BSF. This filter mainly has two quarter-wavelength parallel coupled lines on the top surface of the substrate and a U-shaped SLR coupled to the two parallel lines on the other side of the common substrate [9]. Moreover, to avoid the existing undesired narrow band radio signals, a stub embedded in the U-shaped SLR is used to create an attenuation pole at 5.2 GHz. To show the primary design and frequency response, Figure 2(a) shows the layouts of the UWB filter without the bandstop structure, which the circuit parameters are the same with Figure 1. The electrical length of the microstrip parallel-coupled lines with open circuit are equivalent to quarter-wavelength since the structure can exhibit all-stop response with multiple transmission zeros [6]. The wideband response is excited by the microstrip/U-shaped slotline transition effect due to the 180° phase shift phenomenon [7, 9]. In this study, a stub embedded in the U-shaped SLR is used to create an attenuation pole to avoid the existing undesired narrow band radio signals at 5.2 GHz. The full wave EM simulator IE3D [14] is used

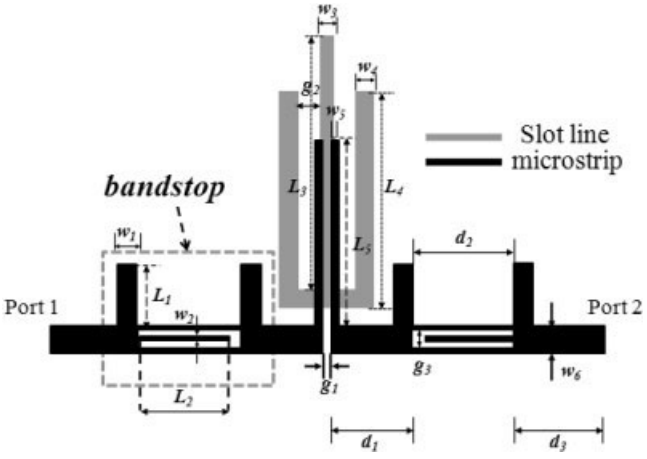

Figure 1 Layouts of the proposed UWB filter with a bandstop filter to improve the stopband

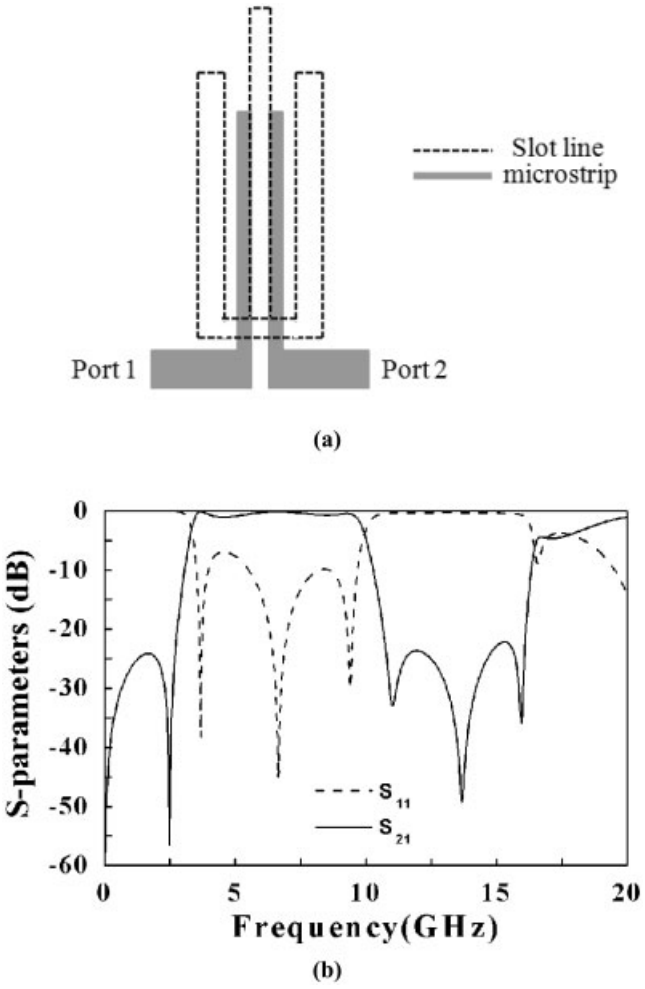

Figure 2 (a) Layouts and (b) simulated frequency response of the UWB filter without the bandstop filter. (The circuit dimensions in this study are $L_3 = 11$, $W_3 = 0.4$, $L_4 = 9.5$, $W_4 = 0.8$, $L_5 = 8.13$, $W_5 = 0.4$, $g_1 = 0.3$, $g_2 = 0.95$, $g_3 = 1$, $d_1 = 3.9$, all scale are united with mm.)

for characterizing the frequency response. The input/output ports are all designed for 50 Ω. When the circuit dimensions in this primary design as without BSF are $L_3 = 11$, $W_3 = 0.4$, $L_4 = 9.5$, $W_4 = 0.8$, $L_5 = 8.13$, $W_5 = 0.4$, $g_1 = 0.3$, $g_2 = 0.95$, $g_3 = 1$, $d_1 = 3.9$, all scale are united with mm, the simulated frequency responses of the UWB BPF is shown in Figure 2(b). It is clearly observed that the proposed UWB filter exhibits the wide passband with the range of 3.3 to 9.8 GHz. Moreover, the multiple transmission zeros appeared at the passband edge at 2.6 and 10.8 GHz improve the selectivity of the proposed UWB BPF. The wide passband is divided into two regions by inserting the stopband of ~5–6 GHz to obtain a lower band of 3.5–5.2 GHz and a higher passband of 6.5–9.7 GHz for UWB specification. However, it is also found that the spurious response is appeared above 15 GHz.

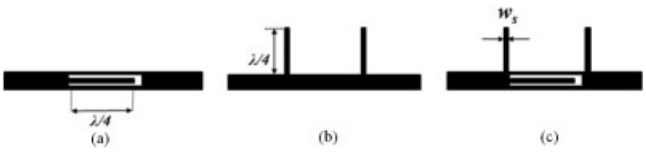

Figure 3 Configurations of (a) the embedded open-stub, (b) conventional open-stub, and (c) the proposed bandstop filter

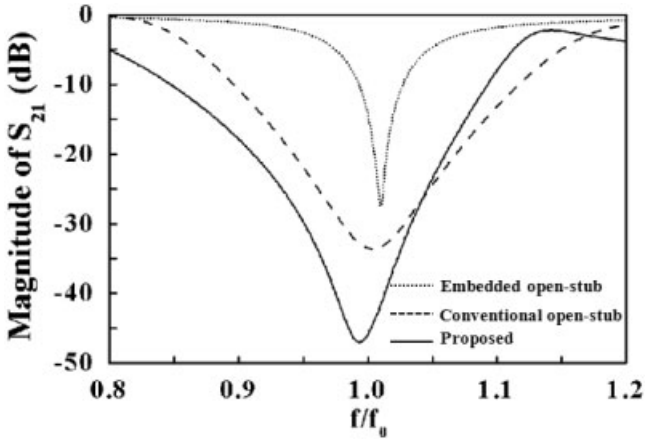

Figure 4 Comparison of the simulated frequency responses for the three structures shown in Figure 3

To obtain a deeper rejection and a wider stopband, a BSF should be proposed to achieve the requirement without affecting the passband performance. Figure 3 show the configurations of three BSFs structures using embedded open stub [11], a pair of shunt open stubs, and the proposed combination of two structures, respectively. The electrical lengths of shunt open stubs and embedded open stub are all designed to be $\lambda_g/4$, where λ_g is the guided wavelength of the microstrip line at the rejection center frequency. Figure 4 shows the comparison of the simulated and normalized frequency response of the three structures in Figure 3. The degrees of rejection for three BSFs are −26, −33, and −48 dB, respectively. It is clearly obtained that the proposed BSF can provide a deeper rejection and a wider stopband response without increasing the circuit size. Figure 5 further shows the simulated frequency response of the proposed BSF with different line widths of the open stubs. When line widths are 0.2, 0.5, and 0.8 mm, the characteristic impedances of the open stub are 137 Ω, 95 Ω, and 75 Ω at the center frequency of 16 GHz, respectively. It is found that a wider stopband response can be obtained by using the open stubs with lower characteristic impedances.

By combing the proposed BSF into the UWB BPF, the comparison of the simulated frequency response of the UWB filter with and without the bandstop structure is shown in Figure 6. With the proposed BSF, a deep and wide stopband rejection greater than 20 dB from 10 to 20 GHz can be obtained. It is also shown the

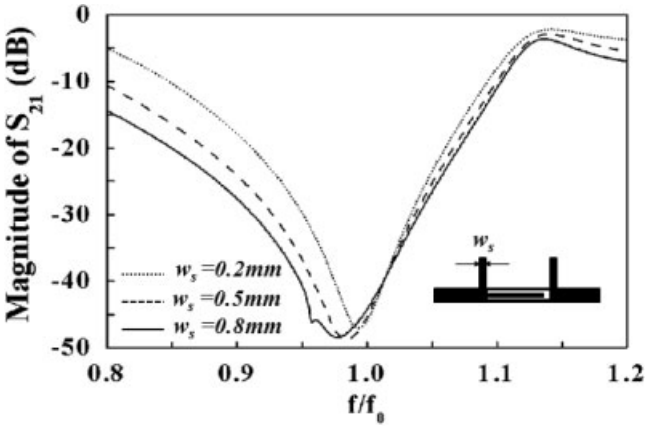

Figure 5 The simulated frequency response of the proposed bandstop structure with different widths of open-stubs

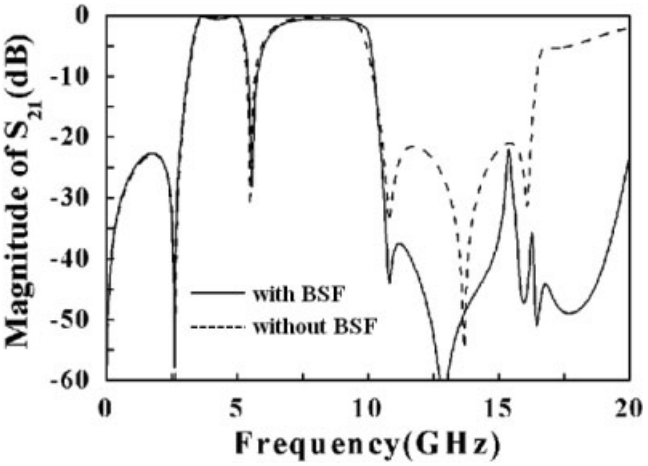

Figure 6 The comparison of the simulated frequency response of the UWB filter with and without the bandstop filter

passband performance of the primary BPF does not vary after connecting the BSF to the primary UWB BPF.

3. EXPERIMENTAL RESULTS AND DISCUSSION

The proposed microstrip UWB BPF is realized on a low cost commercial substrate without using expensive lithography process and measured by an HP8510C Network Analyzer. Figure 7 shows the front view and bottom view photographs of the fabricated filter. The circuit dimensions as shown in Figure 1 are $L_1 = 2.94$, $W_1 = 0.9$, $L_2 = 3.14$, $W_2 = 0.4$, $L_3 = 11$, $W_3 = 0.4$, $L_4 = 9.5$, $W_4 = 0.8$, $L_5 = 8.13$, $W_5 = 0.4$, $W_6 = 1.37$, $g_1 = 0.3$, $g_2 = 0.95$, $g_3 = 1$, $d_1 = 3.9$, $d_2 = 3.37$, and $d_3 = 4.7$, all scale are united with mm. The measured frequency response compared with the EM simulation is displayed in Figure 8. The measured results of the UWB filter at lower passband include a center frequency f_0 of 4.35 GHz, a low insertion loss of 1.9 ± 0.4 dB, a wide bandwidth of 3.5–5.2 GHz (fractional bandwidth, FBW of 39%). The measured results of the UWB filter at higher passband include a center frequency f_0 of 8.1 GHz, a low insertion loss of 2 ± 0.5 dB, and a wide bandwidth of 6.5–9.7 GHz (FBW = 40%). The measured stopband is significantly widened up to 20 GHz with an attenuation level higher than 23 dB. The locations of transmission zeros appear at 2.6, 5.9, and 12.7 GHz, resulting in great improvement of the filter passband

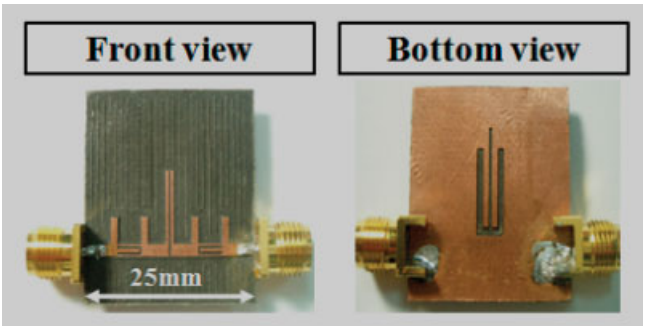

Figure 7 Photographs of the fabricated UWB bandpass filter with the bandstop filter. (The circuit dimensions as shown in Figure 1 in this study are $L_1 = 2.94$, $W_1 = 0.9$, $L_2 = 3.14$, $W_2 = 0.4$, $L_3 = 11$, $W_3 = 0.4$, $L_4 = 9.5$, $W_4 = 0.8$, $L_5 = 8.13$, $W_5 = 0.4$, $W_6 = 1.37$, $g_1 = 0.3$, $g_2 = 0.95$, $g_3 = 1$, $d_1 = 3.9$, $d_2 = 3.37$, and $d_3 = 4.7$, all scale are united with mm.). [Color figure can be viewed in the online issue, which is available at www.interscience.wiley.com]

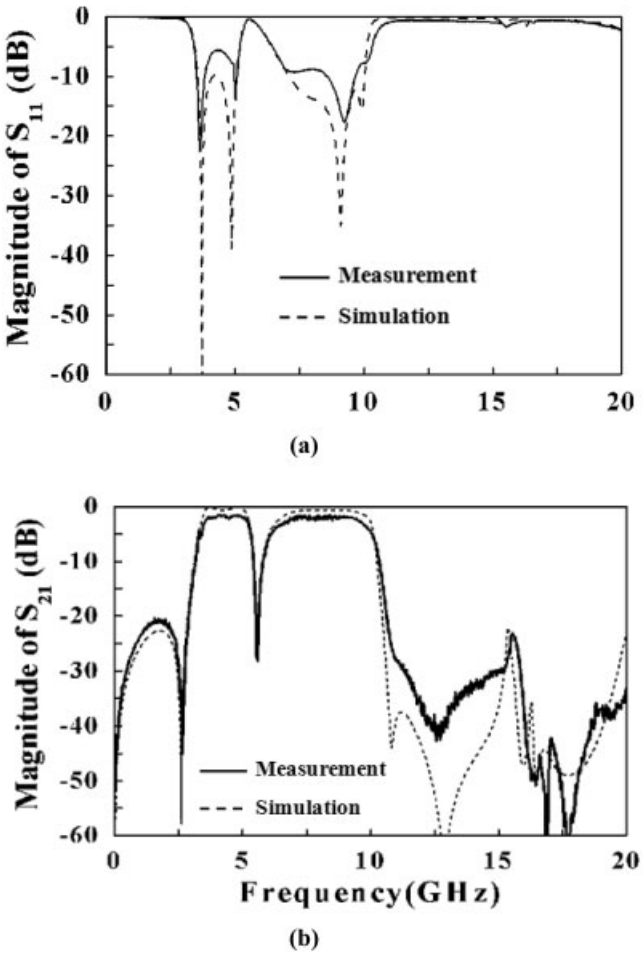

Figure 8 Simulated and measured frequency responses of the proposed UWB filter with the bandstop structure

selectivity. The measured results closely match with the simulated results. The overall size of the fabricated filter is around 25 × 25 mm, indicating the proposed filter exhibits the property of compact size, easy fabrication, and good performance.

4. CONCLUSIONS

In this letter, a UWB BPF with a notch band of 5–6 GHz is proposed. To improve the stopband performance, a bandstop filter using mixed open stubs for suppressing spurious response has been proposed. The proposed BSF shows a deeper rejection and a wider stopband than the conventional open-stub BSF without increasing the circuit size. The proposed UWB BPF shows a lower passband of 3.5–5.2 GHz and a higher passband of 6.5–9.7 GHz as well as 23 dB rejection during the frequency range from 10 to 20 GHz. The measured results of the fabricated UWB BPF actually match with the simulated results.

REFERENCES

1. FCC, Revision of part 15 of the commission's rules regarding ultra-wide-band transmission system, First Note and Order Federal Communication Commission, ET-Docket 98-153, 2002.
2. L. Zhu, S. Sun, and W. Menzel, Ultra-wideband (UWB) bandpass filters using multiple-mode resonator, IEEE Microwave Wireless Compon Lett 11 (2005), 796–798.
3. C.Y. Hung, M.H. Weng, Y.K. Su, R.Y. Yang, and H.W. Wu, Design of compact and sharp rejection UWB BPFs using interdigital stepped impedance resonators, IEICE Electron Lett 1 (2007), 1652–1654.
4. C.Y. Hung, M.H. Weng, R.Y. Yang, and Y.K. Su, Design of the parallel coupled wideband bandpass filters with very high selectivity and wide stopband, IEEE Microwave Wireless Compon Lett 15 (2007), 510–512.
5. R. Li and L. Zhu, Ultra-wideband (UWB) bandpass filters with hybrid microstrip/slotline structures, IEEE Microwave Wireless Compon Lett 11 (2007), 778–780.
6. M.K. Mandal and S. Sanyal, Compact wideband bandpass filter, IEEE Microwave Wireless Compon Lett 1 (2006), 46–48.
7. P. Mondal, M.K. Mandal, and A. Chakrabarty, Compact ultra-wideband bandpass filter with improved upper stopband, IEEE Microwave Wireless Compon Lett 9 (2007), 643–645.
8. N. Thomson and J.S. Hong, Compact ultra-wideband microstrip/coplanar waveguide bandpass filter, IEEE Microwave Wireless Compon Lett 3 (2007), 184–186.
9. C.S. Ye, Y.K. Su, M.H. Weng, R.Y. Yang, and Y.C. Chang, A compact dual-band UWB filter based on the parallel line structure with the slot-line, APMC 2008 Asia-Pacific Microwave Conference, Hong Kong, China, 2008.
10. H. Shaman and J.S. Hong, Ultra-wideband (UWB) bandpass filter with embedded band notch structures, IEEE Microwave Wireless Compon Lett 3 (2007), 193–195.
11. W.H. Tu and K. Chang, Compact microstrip bandstop filter using open stub and spurline, IEEE Microwave Wireless Compon Lett 4 (2004), 268–270.
12. H. Kuan and M.H. Weng, A compact UWB bandpass filter with wide upper stopband using multiple transmission zeros, Microwave Opt Technol Lett 50 (2008), 380–382.
13. M.H. Weng, C.S. Ye, C.Y. Hung, and C.Y. Huang, A novel dual mode bandpass filter with improved spurious response, IEICE Trans Electron Lett 1 (2008), 224–227.
14. Zeland Software, IE3D Simulator, Zeland Software, Feremont, CA, 1997.

MULTIBAND LADDER-SHAPED MONOPOLE ANTENNA FOR DIGITAL TELEVISION AND WIRELESS COMMUNICATIONS

Wen-Chung Liu[1] and Der-Lun Huang[2]
[1] Department of Aeronautical Engineering, National Formosa University, 64, Wenhua Road, Huwei, Yunlin 632, Taiwan; Corresponding author: wencliu@nfu.edu.tw
[2] Institute of Electro-Optical and Materials Science, National Formosa University, 64, Wenhua Road, Huwei, Yunlin 632, Taiwan

Received 3 December 2008

ABSTRACT: *A multiband monopole antenna covering DTV and several popular wireless communications was presented. The antenna fed by a microstrip line comprises a ladder-shaped patch and a notched ground plane. By precisely choosing the dimensions of both the patch and the ground, dual wide continuous impedance bandwidths of 880 MHz (0.51–1.39 GHz) and 1.66 GHz (2.11–3.77 GHz) applicable for multiband wireless operation can be easily achieved. Also, the monopole-like type of radiation patterns and the average gains of about 0.1 and 4.5 dBi, respectively, over the lower and upper operating bands have been obtained.* © 2009 Wiley Periodicals, Inc. Microwave Opt Technol Lett 51: 2124–2127, 2009; Published online in Wiley InterScience (www.interscience.wiley.com). DOI 10.1002/mop.24555

Key words: *multiband; DTV; monopole; wireless communication*